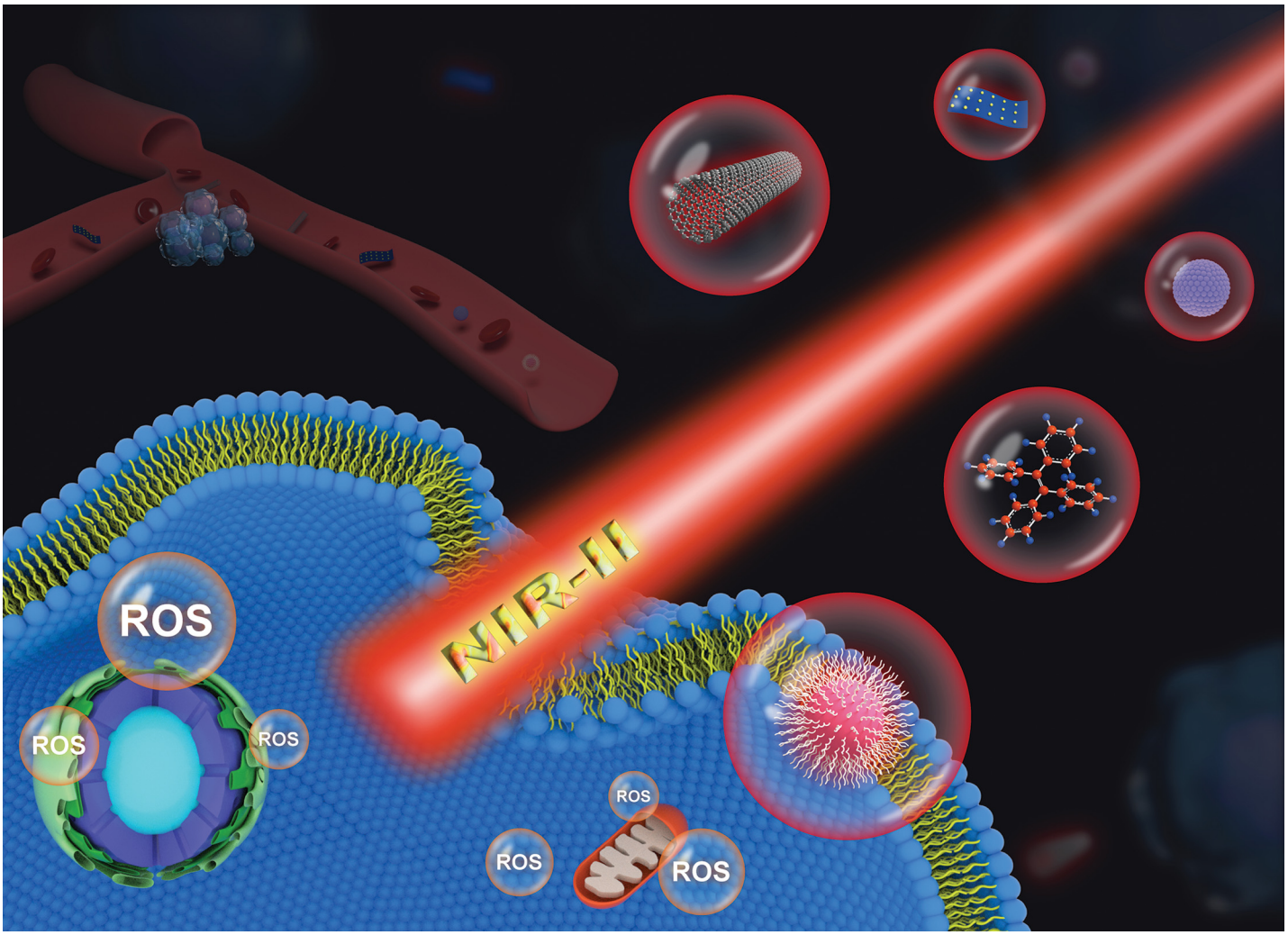

Showcasing review from the Key Laboratory of Molecular Medicine and Biotherapy at the School of Life Sciences at the Beijing Institute of Technology.

Beyond traditional light: NIR-II light-activated photosensitizers for cancer therapy

This review focuses on the recent progress of various NIR-II photosensitizers for photodynamic therapy, as well as briefly presents the ongoing challenges and prospects of the NIR-II photosensitizers for clinical translation.

As featured in:

See Jinfeng Zhang *et al.*, *J. Mater. Chem. B*, 2023, **11**, 8315.

ROYAL SOCIETY OF CHEMISTRY

rsc.li/materials-b

Registered charity number: 207890

Journal of Materials Chemistry B

ROYAL SOCIETY OF CHEMISTRY

REVIEW

View Article Online
View Journal | View Issue

Cite this: *J. Mater. Chem. B*, 2023, **11**, 8315

Beyond traditional light: NIR-II light-activated photosensitizers for cancer therapy

Sa Wang, Chuang Zhang, Fang Fang, Yueyun Fan, Jiani Yang and Jinfeng Zhang *

Received 28th March 2023,
Accepted 14th July 2023

DOI: 10.1039/d3tb00668a

rsc.li/materials-b

With increasing demand for the accurate and safe treatment of cancer, non-invasive photodynamic therapy (PDT) has received widespread attention. However, most conventional photosensitizers are typically excited by short-wavelength visible light (400–700 nm), thus substantially hindering the penetration of light and the therapeutic effectiveness of the PDT procedure. Fortunately, near-infrared (NIR) light (>700 nm), in particular, light in the second near-infrared region (NIR-II, 1000–1700 nm) has a higher upper radiation limit, greater tissue tolerance, and deeper tissue penetration compared with traditional short-wavelength light excitation, and shows considerable potential in the clinical treatment of cancer. Therefore, it is of paramount importance and clinical value to develop photosensitizers that are excited by NIR-II light. In this review, for the first time we focus completely on recent progress made with various NIR-II photosensitizers for cancer treatment *via* PDT, and we briefly present the ongoing challenges and prospects of currently developed NIR-II photosensitizers for clinical practice in the near future. We believe that the above topics will inspire broad interest in researchers from interdisciplinary fields that include chemistry, materials science, pharmaceuticals, and clinical medicine, and provide insightful perspectives for exploiting new NIR-II photosensitizers for biomedical applications.

Key Laboratory of Molecular Medicine and Biotherapy, School of Life Sciences, Beijing Institute of Technology, Beijing 100081, P. R. China.
E-mail: jfzhang@bit.edu.cn

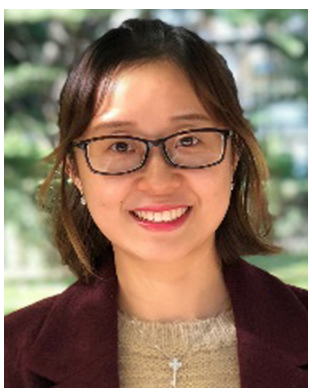

Jinfeng Zhang

Jinfeng Zhang received her M.Sc. degree in organic chemistry in 2013 from the Technical Institute of Physics and Chemistry, Chinese Academy of Sciences, and her PhD from the Department of Biology and Chemistry at City University of Hong Kong, in 2017. Currently, she is an Associate Professor in the School of Life Sciences, Beijing Institute of Technology, China. Her research focuses mainly on the design and fabrication of self-assembled nanomaterials for drug delivery, bioimaging, and the treatment of various diseases, including cancer, inflammation-induced injuries as well as cardiovascular and neurodegenerative diseases.

1. Introduction

Over the past few decades, cancer has emerged as one of the deadliest diseases worldwide.[1,2] Compared with conventional methods of cancer treatment, such as surgery, radiotherapy, and chemotherapy, photodynamic therapy (PDT) is one of the most promising treatment modalities that has improved target specificity and reduced side effects, and has received significant attention from the perspective of both fundamental research and clinical practice.[3–12] According to data from the ClinicalTrials.gov website, more than 500 studies on PDT are ongoing or have been completed, where some of these processes have been clinically approved for cancer therapy.[13] In a typical type-II PDT process, photosensitizers are first activated by absorbing light energy, and they then interact with oxygen (O_2) to generate reactive oxygen species (ROS), which ultimately trigger local or systemic cytotoxicity.[14–17] In this regard, PDT relies on three components: photosensitizers, O_2, and light. Up to now, a variety of chemically and nanotechnologically empowered photosensitizers have been developed to enhance the production of ROS for PDT.[18–27]

Although PDT has been studied widely as a promising treatment for cancer therapy, its wide clinical application has still been greatly limited.[28–31] For example, most conventional photosensitizers are typically excited by visible light (400–700 nm). However, visible light of short wavelengths is not only easily absorbed by biological tissues but also has a limited

tissue-penetration depth.[32–34] Fortunately, due to the relatively weak interaction of near-infrared (NIR) light with biological tissues, photosensitizers excited by light in the first near-infrared window (NIR-I), *i.e.*, in the wavelength range of 700–1000 nm, have drawn widespread attention for biomedical applications.[35–37] Notably, compared with short-wavelength light, excitation in the second near-infrared window (NIR-II; 1000–1700 nm) shows a very weak interaction with biological tissues as well as minimal phototoxicity.[38–43] More importantly, compared with shorter-wavelength light sources (0.33 W cm^{-2} at 808 nm), NIR-II light has a higher maximum permissible exposure (1 W cm^{-2} at 1064 nm) and shows deeper tissue penetration (5–20 mm), and is thus emerging as a more preferable light source for PDT.[44–46] On account of the above advantages, photosensitizers stimulated by NIR-II light are particularly suitable for the treatment of deep-seated cancers. At present, numerous NIR-II-excited imaging and photothermal agents have been developed rapidly, which have been summarized in several previously reported reviews.[47–54] However, there is currently no systematic summary of the NIR-II photosensitizers used for cancer therapy. In this review, we will describe the principle of the photosensitizer mechanism, summarize the recent applications of different types of NIR-II photosensitizers used in cancer treatment (Fig. 1), and discuss the existing challenges in the clinical transformation of photosensitizers based on NIR-II light activation. We believe that this review will provide insightful perspectives and clear prospects towards the rapid development of NIR-II photosensitizers in biomedicine, and will be highly valuable for the exploitation of new photosensitizer materials. This review will also appeal to scientists and researchers in the fields of chemical, physical, material, biological and medical sciences.

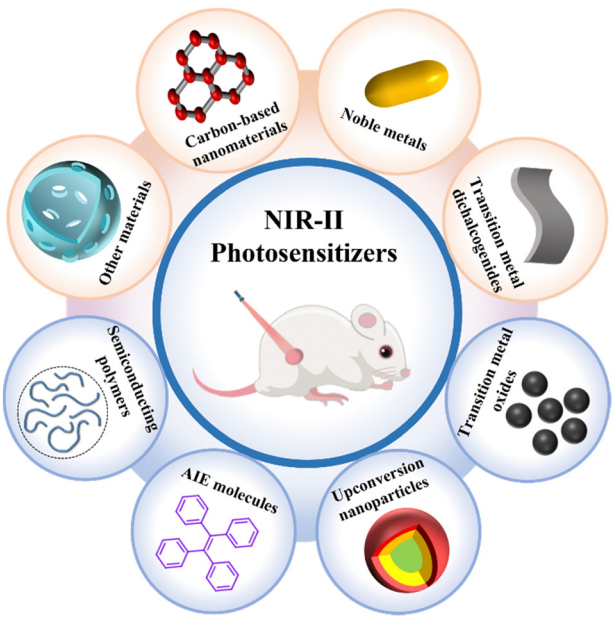

Fig. 1 Schematic illustration of photosensitizers excited by NIR-II light for cancer therapy.

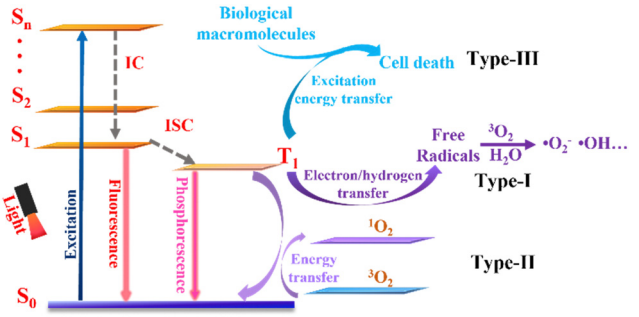

Fig. 2 Three types of photodynamic mechanism exploited for cancer treatment.

2. Mechanism of PDT

Up to now, three types of photodynamic mechanism have been exploited for cancer treatment (Fig. 2). When irradiated with light of the appropriate wavelength, photosensitizers are converted from the ground state (S_0) to an unstable singlet excited state (S_n) followed by a fast internal conversion (IC) process to the lowest singlet excited state (S_1). The excited photosensitizer is unstable and may change from the S_1 state to a more stable excited triplet state (T_1) through intersystem crossing (ISC), thus achieving PDT. According to different photochemical reaction processes, PDT can be divided into three types. For type-I PDT, T_1 reacts directly with the surrounding substrates and transfers electrons/hydrogen atoms to produce free radicals, which may react further with other molecules (*i.e.*, O_2 and water) to generate ROS, which include superoxide anions ($^{\bullet}O_2^-$) and hydroxyl radicals ($^{\bullet}OH$).[55–57] For type-II PDT, the energy of the triplet exciton is transferred to molecular oxygen ($^3O_2$) to produce singlet oxygen ($^1O_2$). Compared with type-II PDT, type-I PDT is less O_2 dependent and is therefore considered to be more suitable for hypoxia conditions. In addition, very recently, Peng's group has provided evidence of a new concept and examples of type-III PDT for cancer treatment, in which type-III photosensitizers can specifically bind and transmit their excitation energy to nucleic acids (*e.g.*, RNA), proteins, and other biological macromolecules in tumor cells upon light irradiation. Consequently, such novel type-III photosensitizers can kill different types of tumor cell directly *via* an O_2-independent pathway.[58]

3. Categories of NIR-II photosensitizer

In order to overcome the limitation of visible-light penetration and apply PDT to deep-seated or large tumors, a variety of functional photosensitizers that can be activated by NIR-II light have been reported. In this section, we will discuss the different types of NIR-II photosensitizer for cancer treatment, which include carbon-based nanomaterials, noble metals, transition metal chalcogenides, transition metal oxides, upconversion nanoparticles, aggregation-induced emission molecules, semiconducting polymers, and other NIR-II photosensitizers. Table 1 summarizes the recently developed NIR-II light-activated photosensitizers used in cancer treatment.

Table 1 Summary of NIR-II light-activated photosensitizers for cancer therapy

Category	Photosensitizer	Laser (nm)	Power	PDT types	Pros	Cons	Ref.
Carbon-based nanomaterials	CDs-NO	1064	0.8 W cm^{-2}	Type-I and type-II	High loading rate Strong NIR absorption	Poor water solubility	66
	Ti_3C_2–Cu–PEG	1064	1 W cm^{-2}	Type-I and type-II	Excellent photon stability Tunable optical properties Easy modification	Dose-dependent toxicity	71
Noble metals	AuNC@HSA/CAT	1064	0.2 W cm^{-2}	Type-I and type-II	Unique physicochemical and optical properties	Difficult to clear	79
	MnO_2/Ag_3SbS_3	1064	1 W cm^{-2}	Type-II	Tunable optical scattering and absorption	Low molar extinction coefficient	80
	Au/Ag NR	1064	1 W cm^{-2}	Type-II			81
Transition metal chalcogenides	FeS_2/CoS_2@PEG	1064	0.8 W cm^{-2}	Type-I	Strong NIR absorption	Disruption of cellular homeostasis Poor water solubility	84
Transition metal oxides	ZrO_{2-x}-B@SiO_2-HA	1064	1 W cm^{-2}	Type-I	Tunable localized surface plasmon resonance	Weak light absorption in the NIR region	86
	PEG-MoO_x	1064	1 W cm^{-2}	Type-II			90
	CeO_{2-x}@HA	1064	1 W cm^{-2}	Type-I			91
Upconversion nanoparticles	TiO_2@UCN/Qr/LA	1060	0.6 W cm^{-2}	Type-I and type-II	Intrinsic upconversion luminescence properties	Limited excitation wavelengths	95
	UCNPs-ZnPc	1532	—	Type-II	Great photostability	Requirement of high laser intensity	96
Aggregation-induced emission molecules	TQ-BTPE	1200	200 J cm^{-2}	Type-II	Unique luminescence enhancement	Limited NIR-II absorption intensity	107
	TPBPy	1000	10 J cm^{-2}	Type-II	Improved ROS generation ability	Low molar extinction coefficient Poor water solubility	111
Organic semiconducting polymers	PTTe	1064	1 W cm^{-2}	Type-I	High photostability Flexible optical properties	Low quantum yield Liver enrichment and long-term retention	116
Layered double hydroxides	LA and LDH	1270	0.5 W cm^{-2}	Type-I	Large specific surface area Tunable chemical composition and structure	Poor stability Difficult to control size and poor repeatability Difficult to clear	118
Mesoporous materials	ER-$HMCu_{2-x}S$/CXB	1064	0.8 W cm^{-2}	—	Porous structure and surface area	Poor dispersion	121
	TCLP	1064	0.8 W cm^{-2}	Type-I and type-II	Easy functionalization pH response degradation	Complex synthesis process	122

3.1. Carbon-based nanomaterials

Compared with other traditional photosensitizers, carbon-based nanomaterials have become increasingly attractive in PDT due to their high loading rate, strong NIR absorption, excellent photon stability, tunable optical properties, easy modification and functionalization, and low toxicity.[59–63] Among them, carbon dots and MXene nanomaterials have been used widely as NIR-II photosensitizers for PDT in recent years.

3.1.1. Carbon dots. Carbon-based nanomaterials with diameters between 1 and 10 nm are commonly referred to as carbon dots (CDs), and are generally considered to be core–shell structures. The outer layer of the graphite core usually contains rich functional groups, which include $–NH_2$, –OH, and –COOH. Such hydrophilic groups endow the CDs with good water solubility and the capability of further functionalization.[64,65] In addition, due to their wide absorption spectra, tunable emission region, photostability, and good biocompatibility, recent studies have shown that CDs have potential applications in NIR-II PDT. For example, Wang and co-authors used methylene blue (MB) as a carbon source, H_2SO_4 as an oxidant and a dehydration (carbonization) agent to synthesize CDs *via* a hydrothermal method for 1064 nm laser-activated PDT.[66] The results showed that the aromatic structure of MB and the heteroatoms of the carbon source have an important impact on the ROS generation performance of the as-synthesized CDs. In addition, due to the hydrothermal process, a large number of –OH groups were retained on the surface of the CDs, which could then be subject to a simple nitrification reaction to induce nitrification of the CDs (CDs-NO). More interestingly, the CDs-NO could release NO for gas therapy (GT) in the presence of glutathione (GSH) which is overexpressed in the tumor microenvironment. Under NIR-II irradiation, the ROS can capture NO rapidly and form $ONOO^-$ free radicals with a high cytotoxicity. Besides, the depletion of GSH can alleviate the antioxidant system in the tumor microenvironment, which is beneficial for increasing the oxidative stress of PDT. Finally, the synergetic therapy can arouse an immune response and effectively inhibit tumor metastasis.

3.1.2. Metal carbides and nitrides. MXene is a two-dimensional material formed of transition metal carbides and nitrides or carbonitrides. In recent years, MXene nanosheets have become an ideal carrier candidate for research into tumor phototherapy due to their large specific surface area, easy functionalization, and uniform composition.[67–70] Ti_3C_2, as a common MXene nanosheet, is usually used to load drugs or metal nanoparticles for combined tumor treatment, although it

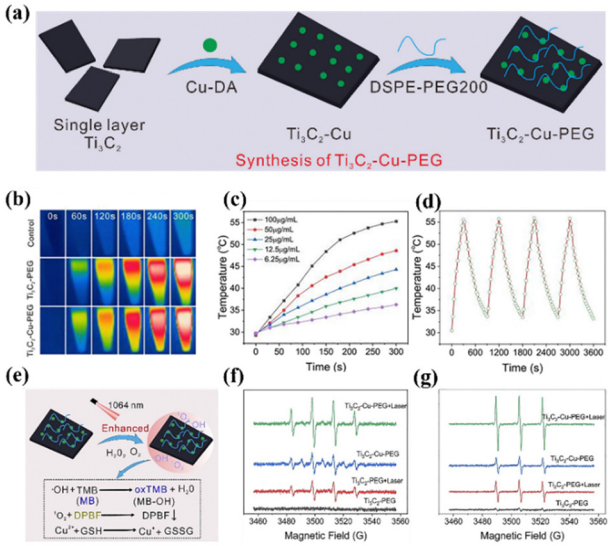

Fig. 3 (a) Schematic illustration of the preparation of Ti_3C_2–Cu–PEG. (b) Temperature variation infrared thermal images of Ti_3C_2–Cu–PEG (100 μg mL^{-1}). (c) Ti_3C_2–Cu–PEG at different concentrations under 1064 nm irradiation. (d) Recycling–heating profiles of Ti_3C_2–Cu–PEG (1064 nm, 1 W cm^{-2}) for four laser on/off cycles. (e) Schematic diagram of the detection of ROS generated by Ti_3C_2–Cu–PEG and its GSH consumption. (f) Electron spin resonance (ESR) spectra of •OH with or without laser irradiation. (g) ESR spectra of $^1O_2$ with or without laser irradiation. Reproduced with permission from ref. 71. Copyright 2022, De Gruyter.

suffers from poor stability against O_2 and water. Zhang *et al.* proposed and fabricated a biocompatible and O_2-resistant Cu-decorated Ti_3C_2 nanocomposite (Ti_3C_2–Cu–PEG), which could effectively consume the GSH, responding smartly to NIR-II light to achieve photothermally enhanced PDT (Fig. 3a).[71] Specifically, after irradiation with 1064 nm laser light (1 W cm^{-2}) for 5 min, the temperature of Ti_3C_2–Cu–PEG reached 55.8 °C, indicating a good photothermal performance (Fig. 3b–d). Attractively, the Ti_3C_2–Cu–PEG not only reacted with O_2 to generate $^1O_2$ *via* NIR-II light radiation but also catalyzed the endogenous H_2O_2 to produce •OH (Fig. 3e–g). Furthermore, Ti_3C_2–Cu–PEG could consume GSH to promote oxidative stress, finally achieving NIR-II-triggered PDT synergistic anti-tumor therapy both *in vitro* and *in vivo*.

3.2. Noble metals

In recent years, noble metal nanomaterials have attracted wide interest because of their unique physicochemical and optical properties.[72–74] Among them, gold (Au) and silver (Ag) show unique size- and shape-dependent optoelectronic characteristics. Therefore, it is possible to adjust the optical properties of noble metal materials by changing the size and shape, enhancing their therapeutic properties as photosensitizers.[75–78] In addition, the possibility of further chemical modification improves their bioavailability, making noble metal nanomaterials a potent candidate for the clinical treatment of cancer.

3.2.1. Gold nanoparticles. In 2018, Liu's group developed a novel and multifunctional photosensitizer that simultaneously achieves tumor hypoxia relief, *in vivo* fluorescence imaging, and NIR-II light-activated PDT.[79] In this study, they used human serum albumin (HSA) and catalase (CAT) to co-modify alkyl thiolated gold nanoclusters (AuNCs), namely AuNC@HSA/CAT nanoparticles. In the AuNC@HSA/CAT system, HSA greatly promoted the physiological stability of the nanoparticles, and the AuNCs could efficiently generate •OH and $^1O_2$ under 1064 nm light irradiation. The coating of CAT triggered the degradation of endogenous tumor H_2O_2 to produce O_2, thus improving the effect of PDT through relieving tumor hypoxia.

3.2.2. Silver nanoparticles. As a typical example of silver-based semiconductors, Ag_3SbS_3 nanoparticles with a narrow band gap (1.5–1.7 eV) exhibit superb optical absorption in the NIR-II window, show negligible invasiveness, and no accumulation of multidrug resistance, displaying an excellent feasibility for NIR-II PA imaging, photothermal therapy (PTT) and PDT. As shown in Fig. 4a, Wang *et al.* synthesized Ag and Ag_3SbS_3 nanoparticles using a typical hydrothermal method, then the Ag_3SbS_3 NPs were decorated with PEG and loaded with MnO_2 to prepare MnO_2/Ag_3SbS_3 (MA).[80] Intriguingly, the tumor microenvironment could trigger the degradation of MA into Mn^{2+} ions and ultrasmall Ag_3SbS_3 nanoparticles (Fig. 4b), which can be rapidly excreted *via* liver and kidney pathways, avoiding their accumulation in normal tissues. The released Mn^{2+} ions could catalyze H_2O_2 to generate •OH through a Fenton-like reaction (Fig. 4c). As shown in Fig. 4d, under different pH conditions and 1064 nm laser irradiation, the generation of $^1O_2$ in the MA solution is detected using the 1,3-diphenylisobenzofuran (DPBF) probe sensor. The results showed that acidic conditions were helpful to promote the formation of $^1O_2$. In addition, MA could constantly deplete GSH and produce O_2 for enhancing the efficiency of chemodynamic therapy (CDT) and PDT. In another study, Jin *et al.* reported a corn-like Au/Ag nanorod (Au/Ag NR) for NIR-II activated PDT/PTT, which could further reprogram the immunosuppressive tumor microenvironment and sensitize tumors to immune checkpoint blocking (ICB) antibodies, especially aCTLA4, for synergistic antitumor treatment.[81] The surface plasmon resonance (SPR) band of Au/Ag NRs could be adjusted to the NIR-II region by tuning the

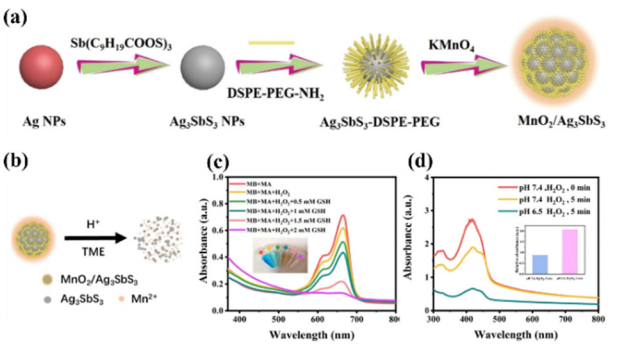

Fig. 4 (a) Schematic diagram of MnO_2/Ag_3SbS_3 preparation. (b) Ag_3SbS_3 and Mn^{2+} were released from MnO_2/Ag_3SbS_3 under acid stimulation of the tumor microenvironment. (c) •OH generated from MA nanoparticles was detected by MB. (d) $^1O_2$ generation by MA nanoparticles at different pH values. Reproduced with permission from ref. 80. Copyright 2022, American Chemical Society.

thickness of the Ag shell. The Au/Ag NRs could generate hyperthermia and ROS under 1064 nm laser irradiation and consequently trigger the immunogenic cell death (ICD) of cancer cells by increasing the T cell invasion of tumors, converting the cold tumor microenvironment into a hot microenvironment. Finally, Au/Ag NR-mediated NIR-II PDT/PTT synergized with ICB antibodies showed a powerful immunological memory result, preventing tumor recurrence.

3.3. Transition metal chalcogenides

Due to their narrow band gap, transition metal chalcogenides show a strong harvest in the NIR range and have been applied extensively in photocatalysis as well as phototherapy (PDT and PTT).[82,83] As shown in Fig. 5a, Wang *et al.* used Fe–Co layered double hydroxides (LDHs) as precursors to prepare the Z-scheme nanostructure FeS_2/CoS_2@PEG (FCs@PEG).[84] The Z-scheme mechanism endows FCs@PEG with a high redox potential of photogenerated charge to oxidize water into O_2 and subsequently capture O_2 to produce $^{\bullet}O_2^-$ (Fig. 5b). Importantly, FCs@PEG exhibited significant NIR-II absorption and an excellent photothermal conversion efficiency of 50.5% upon 1064 nm irradiation. Fig. 5 shows that the high temperature provides additional energy to achieve the co-excitation of CoS_2 (1.37 eV) and FeS_2 (1.16 eV) through 1064 nm laser irradiation (1.16eV). Moreover, the as-fabricated FCs@PEG exhibited improved simulated CAT and peroxidase (POD) activities due to the lower resistance for charge transfer in the heterostructure, efficiently catalyzing endogenous H_2O_2 into O_2 and $^{\bullet}OH$, thereby alleviating hypoxia (Fig. 5c). Finally, the tumor treated with FCs@PEG and NIR-II light was almost ablated, demonstrating the excellent synergistic antitumor effect of PDT/PTT.

3.4. Transition metal oxides

Semiconductor nanomaterials based on transition metal oxides have garnered extensive attention due to their tunable localized surface plasmon resonance (LSPR).[85] Considerable efforts have been made using plasmonic semiconductor nanomaterials for NIR-II light-activated PDT. Zhu and co-authors discovered a tumor-targeting ZrO_2-based phototherapeutic agent to achieve NIR-II PA imaging-guided PTT/PDT synergistic phototherapy, where boron-doped O_2-deficient zirconia (ZrO_{2-x}-B) was formed *via* $NaBH_4$ reduction, and was functionalized further with a layer of SiO_2 covalently linked with hyaluronic acid (HA), termed as ZrO_{2-x}-B@SiO_2-HA (Fig. 6a).[86] The ZrO_{2-x}-B@SiO_2-HA agent exhibited full spectral absorption properties due to the oxygen vacancies and boron doping (Fig. 6b), enabling high NIR-II photothermal conversion and significant ROS generation (Fig. 6c). Fig. 6d illustrates the mechanism of NIR-II light-induced ROS production, in which the light firstly irradiates the ZrO_{2-x}-B@SiO_2-HA to produce pairs of electrons and holes. Notably, the oxygen vacancies can be used as trapping sites of photogenerated electrons to enhance charge separation. Then, the generated electrons and holes can combine with water and O_2 on the surface of ZrO_{2-x}-B to generate $^{\bullet}O_2^-$ and $^{\bullet}OH$, respectively. The mechanism was further confirmed using ESR spectroscopy, as shown in Fig. 6e, which shows the presence of oxygen vacancies in ZrO_{2-x}-B@SiO_2-HA. Furthermore, the decoration of HA made ZrO_{2-x}-B@SiO_2-HA with a water dispersion ability as well as a targeting ability toward CD44 overexpressed on tumor cells. Hence, the as-prepared ZrO_{2-x}-B@SiO_2-HA reveals accurate NIR-II laser-activated cancer-targeting PTT/PDT.

In addition to ZrO_2, oxygen-deficient molybdenum oxide nanoparticles (MoO_x NPs) can also be utilized in PTT/PDT

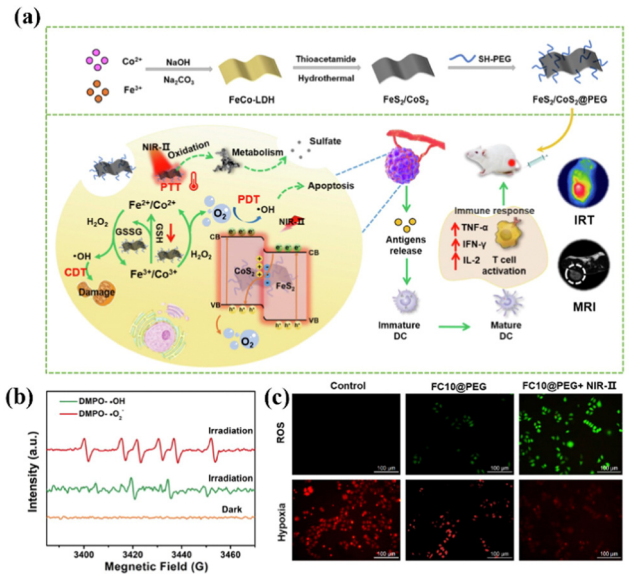

Fig. 5 (a) Schematic illustration of the synthesis of FeS_2/CoS_2 nanosheets using Fe–Co LDHs as the precursor. (b) ESR spectra of FCs@PEG trapped by DMPO under 1064 nm irradiation. (c) Detection of ROS production with DCFH-DA. Reproduced with permission from ref. 84. Copyright 2022, Elsevier.

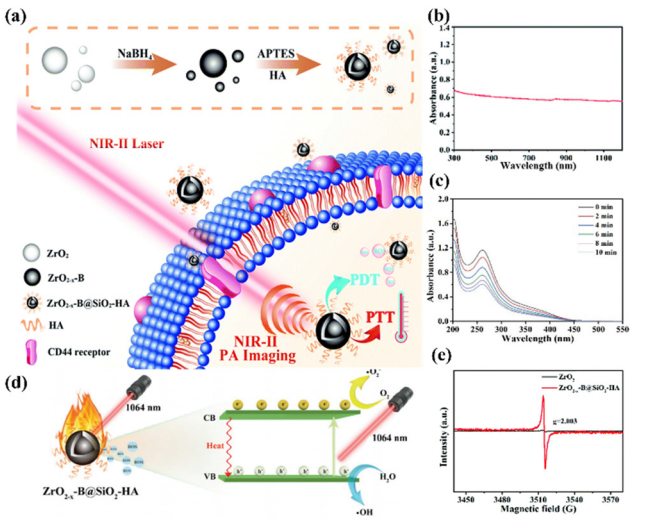

Fig. 6 (a) Schematic of the fabrication of ZrO_{2-x}-B@SiO_2-HA for NIR-II PA imaging-mediated tumor-targeting therapy. (b) UV-vis-NIR spectrum of ZrO_{2-x}-B@SiO_2-HA. (c) Nitro blue tetrazolium was employed to test $^{\bullet}O_2^-$ of ZrO_{2-x}-B@SiO_2-HA under 1064 nm laser irradiation. (d) Schematic of the PTT/PDT mechanism of ZrO_{2-x}-B@SiO_2-HA. (e) ESR detected the oxygen vacancies of ZrO_{2-x}-B@SiO_2-HA. Reproduced with permission from ref. 86. Copyright 2020, Royal Society of Chemistry.

synergistic therapy because the LSPR of the MoO_x NPs can be regulated to the NIR window by adjusting its chemical composition.[87–89] Yin *et al.* reported PEGylated MoO_x nanoparticles (PEG-MoO_x NPs), which were prepared through a facile hydrothermal method.[90] The PEG-MoO_x NPs exhibited extensive absorption in the NIR region and a significant photothermal conversion efficiency under both 808 nm and 1064 nm light irradiation. Interestingly, the PEG-MoO_x NPs could only conduct limited PTT of cancer cells when exposed to 808 nm irradiation, whereas under irradiation at 1064 nm the PEG-MoO_x NPs could not only efficiently convert NIR light into heat but also were sensitized to form ROS. In recent years, oxygen-deficient cerium oxide (CeO_{2-x}) has also been studied in the field of NIR-II PDT where the introduction of oxygen vacancies can reduce the band gap of CeO_{2-x} and enable its optical absorption located in the NIR region. Li *et al.* first used CeO_{2-x} with plenty of oxygen vacancies as a single NIR-II light-triggered nanotheranostic for sonodynamic therapy (SDT)-enhanced phototherapy.[91] CeO_{2-x}, with surface crystalline disorder, exhibited a broad absorption in the NIR-II region. In addition, CeO_{2-x} contains a large number of oxygen defects, which can facilitate the separation of holes and electrons under ultrasound, significantly enhancing the efficacy of its photothermal and photodynamic capabilities. *In vitro* and *in vivo* experiments confirmed that CeO_{2-x}@HA showed an outstanding therapeutic effect of SDT-enhanced PDT/PTT upon NIR-II laser irradiation, realizing complete tumor ablation with good biocompatibility.

3.5. Upconversion nanoparticles

Rare-earth doped upconversion nanoparticles (UCNPs) have emerged as one of the most promising inorganic nanomedicines for cell labeling, bioimaging, and cancer therapy owing to their intrinsic upconversion luminescence (UCL) properties of low-energy NIR light into high-energy ultraviolet or visible light, excellent photostability, and low toxicity.[92–94] In particular, compared with carbon-based materials and organic fluorophores, UCNPs are highly suitable as NIR-II photosensitizers because they are inherently activated by NIR laser irradiation. Recently, Zhang and colleagues fabricated a NIR-II-excited therapeutic agent formed of ytterbium (Yb)- and erbium (Er)-doped titanium dioxide nano-shovel/quercetin/l-arginine (TiO_2@UCN/Qr/LA) on a titanium bone implant (Fig. 7a), in which the doped rare-earth elements enabled up-conversion to generate ROS upon illumination with a 1060 nm laser.[95] Encouragingly, the introduction of rare-earth elements not only enhanced the optical absorption and reduced the band gap but also produced abundant oxygen vacancies to promote the separation of electrons and holes, thus improving the photocatalytic performance and the resultant ROS generation ability (*e.g.*, $^1O_2$ and $^\bullet$OH) of the TiO_2@UCN/Qr/LA under NIR-II irradiation (Fig. 7b and c). More intriguingly, the generated ROS further catalyzed LA to NO to promote therapy. Both *in vitro* and *in vivo* evaluations demonstrated that TiO_2@UCN/Qr/LA could ablate tumors and eliminate biofilms *via* NIR-II PDT combined with other therapies.

Besides, to solve the problem that the excitation band of the upconversion material is limited to short wavelengths

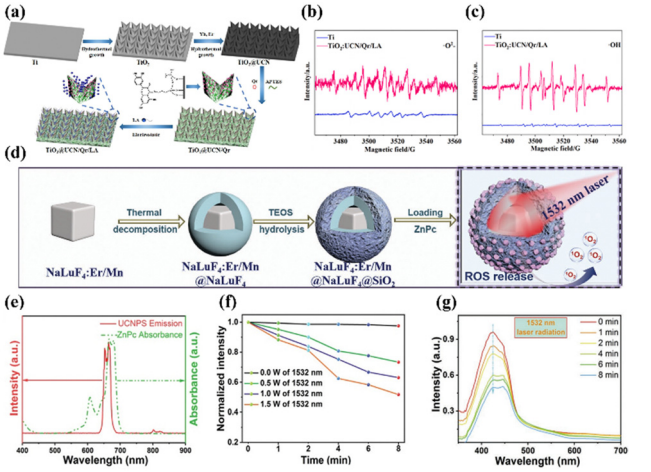

Fig. 7 (a) Preparation process of the TiO_2@UCN/Qr/LA nano-shovel on the Ti implant. Detection of (b) $^1O_2$ and (c) $^\bullet$OH from Ti and TiO_2@UCN/Qr/LA with DMPO. Reproduced with permission from ref. 95. Copyright 2022 Elsevier. (d) Preparation of Er-sensitized UCNPs and the process of activating PDT with 1532 nm light. (e) Normalized absorbance spectrum of ZnPc and UCL spectrum of the UCNPs. (f) ROS generation *via* irradiation at different light intensities. (g) ROS release with 1532 nm laser radiation. Reproduced with permission from ref. 96. Copyright 2022, John Wiley & Sons Inc.

(<1000 nm) and thus expand its application in the biomedical field, Bi *et al.* introduced Er^{3+} as a sensitizer to construct novel Er/Mn co-doped NIR-II photo-responsive UCNPs, which were further loaded with the zinc phthalocyanine (ZnPc) photosensitizer (Fig. 7d).[96] NIR-II-excited PDT can be easily achieved *via* a typical Förster resonance energy transfer (FRET) process in which energy can be efficiently transferred from the UCNPs to the ZnPc, because the emission spectrum of the Er-sensitized UCNPs overlaps well with the absorbance band of ZnPc (Fig. 7e). Subsequent experimental results demonstrated that a significant ROS signal can be detected upon 1532 nm laser irradiation, and the intensity was related to the laser power density (Fig. 7f and g). In addition, by tuning the concentration of Mn^{2+} in the Er/Mn co-doped UCNPs, their crystal phase, size, and emitting colour were readily manipulated. Subsequently, the inert shell of the Er/Mn co-doped UCNP can overcome surface defects, further enhancing its red UCL intensity by ~8-fold. In short, this work successfully achieved NIR-II light-activated red upconversion bioimaging and PDT through the loading of the ZnPc photosensitizer for the first time, providing a novel method for the application of NIR-II light-activated single-band red emissive UCNPs in biomedicine.

3.6. Aggregation-induced emission molecules

So far, several conventional organic molecules, such as squaric acid and cyanine dyes, have been exploited as NIR-II photosensitizers.[97,98] However, these conventional organic dyes suffer from fluorescence quenching effects upon aggregation to form nanoparticles with poor photostability, which significantly impede their wider bio-applications.[99,100] Inspiringly, over the past two decades, molecules with aggregation-induced emission

(AIE) characteristics that exhibit unique luminescence enhancement properties, due to the restriction of molecular motion in the aggregated state, have attracted great attention in the field of biological imaging.[101–103] More importantly, their light-triggered ROS-generating ability is substantially improved in the aggregated state, making AIE molecules promising photosensitizers for PDT applications.[104,105] However, the absorption and emission of most AIE molecules are in the visible-light range, which severely limits their practical application in deep tissue therapy. Fortunately, AIE molecules with favourable two-photon absorption features can be excited by concurrently absorbing two long-wavelength photons, thus providing great prospects for building AIE photosensitizers for NIR-II PDT.[106] For example, Wang *et al.* designed an AIE photosensitizer (TQ-BTPE) with long two-photon absorption and significant $^1O_2$ production for NIR-II PDT (Fig. 8a).[107] TQ-BTPE displayed bright NIR two-photon fluorescence (about 700 nm) and satisfactory $^1O_2$ generation upon excitation at the NIR-II wavelength of 1200 nm. Noticeably, TQ-BTPE exhibited a much greater $^1O_2$ production ability than that of chlorin e6 (Ce6), suggesting its efficient two-photon photosensitization (Fig. 8b). This work exhibits the first example of two-photon activated organic photosensitizers for NIR-II PDT, and provides new insights for the development of NIR-excited photosensitizers.

In addition, the construction of a donor–acceptor (D–A) structure is one of the most effective methods to design photosensitizers with long-wavelength absorption, where the strong intramolecular charge transfer in the D–A structure will promote a redshifted absorption and enhance the resultant long-wavelength two-photon absorption.[108–110] For instance, Luo's group synthesized an AIE photosensitizer (TPBPy) with a donor–π–receptor (D–π–A) core structure for NIR-II PDT.[111] On the one hand, the D–π–A structure could be beneficial for redshifting the absorption peak, endowing the TPBPy with an NIR-II light excitation capability. Furthermore, the conjugated system could reduce the energy gap considerably between the singlet excited state and the triplet excited state, further improving the ISC process and significantly enhancing the $^1O_2$ production ability. To this end, tumor growth was greatly inhibited after treatment *via* TPBPy-mediated NIR-II two-photon PDT.

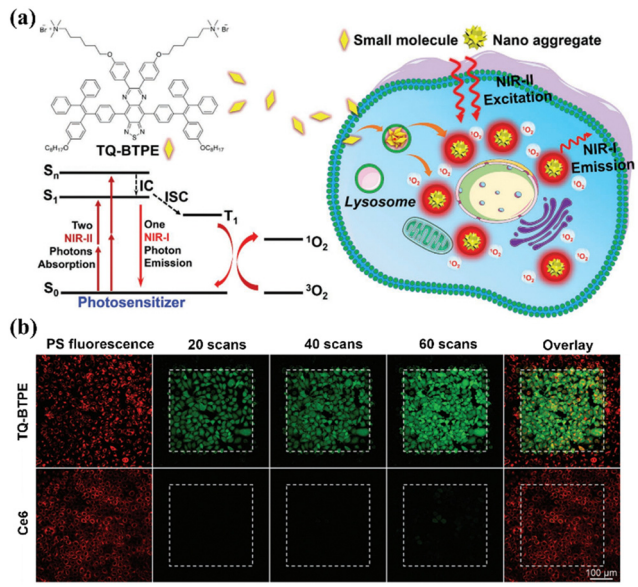

Fig. 8 (a) Chemical structure of TQ-BTPE and schematic of the NIR-II light-activated two-photon photodynamics used to kill tumor cells. (b) TQ-BTPE and Ce6 were irradiated with an NIR-II laser to generate $^1O_2$ in cells, with scanning at different time points. Reproduced with permission from ref. 107. Copyright 2020, John Wiley & Sons Inc.

3.7. Organic semiconducting polymers

Compared with traditional small-molecule-based photosensitizers, organic semiconducting polymers (OSPs) have unique advantages of high photostability, flexible optical properties, and good biocompatibility due to the entirely organic constituents, which make OSPs more promising for *in vivo* phototherapy.[112–115] For instance, Wen *et al.* constructed three semiconducting polymers, *i.e.*, PTS, PTSe, and PTTe, that showed strong absorption in the NIR-II region through different D–A molecular structures, in which thiophenoindole (T) served as the strong electron-absorbing unit and thiophene (S), selenophenol (Se) or benzene telluride (Te) acted as the donor unit, respectively (Fig. 9).[116] More attractively, by introducing heavy atoms (selenium and tellurium) into the molecular skeleton, the rate constant of ISC (k_{ISC}) was improved markedly to generate triplet excitons, which is favorable for yielding ROS. Besides, the Gibbs free energy change between PTS, PTSe, or PTTe and $^3O_2$ was less than zero, which facilitated type-I PDT *via* intermolecular electron transfer. In addition, the PTTe nanoparticles efficiently produced more $^{\bullet}O_2^-$ and a higher photothermal conversion efficiency than the other two nanoparticles upon NIR-II light irradiation, showing outstanding type-I PDT synergetic therapy performance both *in vitro* and *in vivo*.

3.8. Other materials as photosensitizers

In addition to the above-mentioned carbon-based nanomaterials, noble metals, transition metal chalcogenides, transition metal

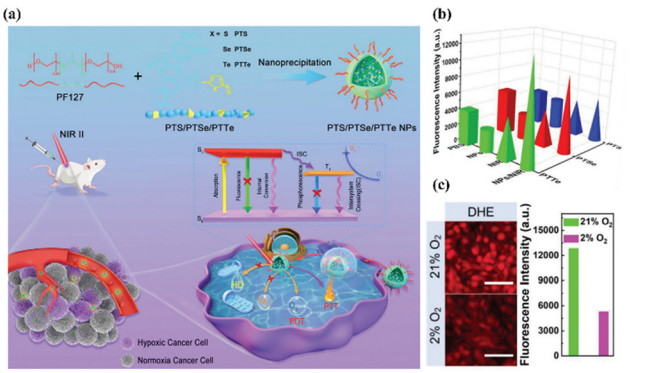

Fig. 9 (a) Synthesis of PTS, PTSe, and PTTe nanoparticles, and their application in NIR-II PDT/PTT synergistic cancer therapy under hypoxic conditions. (b) $^{\bullet}O_2^-$ production of different semiconducting polymers with or without the NIR-II irradiation. (c) $^{\bullet}O_2^-$ production of PTTe nanoparticles was detected under normoxia or hypoxic conditions. Scale bar, 100 μm. Reproduced with permission from ref. 116. Copyright 2022, John Wiley & Sons Inc.

oxides, UCNPs, AIE molecules, and semiconducting polymers, there are some other NIR-II photosensitizers, such as two-dimensional layered double hydroxides (LDHs) and mesoporous materials. As a typical two-dimensional nanomaterial, LDHs have a large specific surface area and unique physical and chemical properties. In recent years, due to their adjustable chemical composition and good biocompatibility, LDHs have attracted widespread research attention in the biomedical field.[117] Yang and co-authors coupled *Lactobacillus acidophilus* probiotics with CoCuMo-LDH nanosheets (LA and LDH) to construct tumor-microenvironment-responsive photosensitizers for accurate NIR-II PDT.[118] Specifically, the hypoxia tropism properties of LA endow LA and LDH with excellent tumor targeting. In addition, the low pH ($\sim$5.4) of LA metabolites and GSH transform the CoCuMo-LDH nanosheets into amorphous states, significantly improving the production of $^1O_2$ upon 1270 nm laser irradiation, with a quantum yield of 0.75/1.06. This work provides an excellent strategy for the *in situ* activation of photosensitizers to achieve accurate NIR-II PDT.

Mesoporous materials, mesoporous silicas in particular, are used widely in anti-tumor drug-delivery studies due to their porous structure and surface area, easy surface functionalization, and pH response degradation.[119,120] Very recently, some studies have shown that mesoporous nanoparticles can be used in NIR-II PDT. Wan *et al.* obtained ER-HMCu_{2-X}S/CXB by modifying hollow mesoporous $Cu_{2-X}S$ with *p*-toluenesulfonamide (for endoplasmic reticulum (ER) targeting) and loading it with a vascular inhibitor (celecoxib; CXB).[121] The as-prepared ER-HMCu_{2-X}S showed good synergistic treatment of NIR-II-mediated PDT/PTT as well as induced ICD for triple-negative breast cancer ablation, which also greatly inhibited cancer recurrence. In another study by Zhang *et al.*, black mesoporous titanium (H-TiO_2) was first loaded with chloroperoxidase (CPO) and β-lapachone (β-Lap), and then encapsulated with polyacrylic acid (PAA), to form TCLP nanocomposites.[122] Notably, the H-TiO_2 within the TCLP could be used as a NIR-II-activated photothermal agent and photosensitizer, while the β-Lap could enhance the $^1O_2$ formation from CPO due to an increase in H_2O_2. As a result, the TCLP mediated the production of plenty of ROS and significantly overcame heat shock protein (HSP)-dependent tumor resistance, thereby improving the synergistic anti-tumor effect of NIR-II PTT/PDT.

4. Conclusion and outlook

As a promising cancer treatment modality, PDT, with non-invasiveness and remarkable therapeutic selectivity, has been developed significantly and implemented in clinical practice. However, so far, most traditional photosensitizers are still excited by short-wavelength visible light, which not only substantially discounts their therapeutic performance but also severely limits their widespread use, especially for the treatment of deep tumors. Recently, great progress has been made in NIR-II-activated photosensitizers that use a long-wavelength light from 1000 to 1700 nm for PDT, and these exhibit minimal

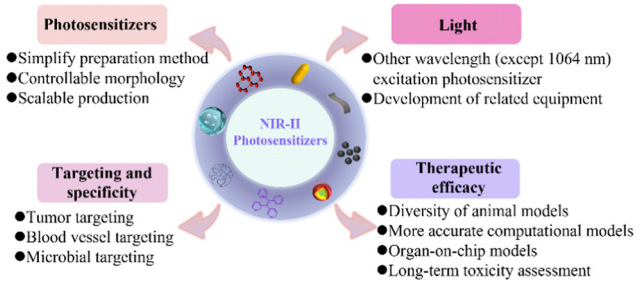

Fig. 10 Typical ongoing challenges for enhancing the clinical translation of NIR-II photosensitizers.

scattering loss, deeper tissue penetration, an improved photon-capturing ability, and satisfactory biosafety. In this review, we describe the latest principles of the photosensitizer mechanism, and, for the first time, summarize the various types of NIR-II-excited photosensitizer as well as their applications in cancer therapy.

Despite the encouraging features of NIR-II PDT for cancer treatment, such cutting-edge therapeutic technology is still in its infancy, and several major concerns remain to be resolved for further clinical applications (Fig. 10).

(1) In the clinical transformation of NIR-II photosensitizers, the complex synthesis steps required not only lead to increased production costs but also increase the toxicity of the photosensitizers, and there are still problems regarding their large-scale and repeatable synthesis.[123] Moreover, the instability of nanomaterials requires strict storage conditions, which also hinders the clinical application of NIR-II photosensitizer-based nanomedicines. In addition, the morphology, size and surface charge of nanomaterials have important effects on blood circulation, tumor penetration and accumulation. Therefore, simple preparation methods, controllable morphologies, and the large-scale production of NIR-II photosensitizer molecules or nanomaterials are particularly important and require further exploration.

(2) NIR-II photosensitizers have poor specificity for tumors, which may lead to low treatment efficiencies and potential damage to other healthy tissues. Several studies have shown that the tumor microenvironment promotes the development of malignant tumors and becomes a potential therapeutic target. Researchers have designed new targeted antitumor photosensitizers that are based on the general physiological features of the tumor microenvironment. However, pH values, enzymes, and reducing agents in clinical applications may change, leading to poor responsiveness and low sensitivity.[124] Following the in-depth study of tumors, strategies based on blood-vessel-targeted anticancer therapy are being developed. Photosensitizers can be selectively accumulated in the tumor vasculature by targeting blood vessels, where photosensitizers are more likely to obtain oxygen to alleviate the hypoxia of PDT, and achieve tumor-specific killing by causing vessel constriction and thrombus. However, tumor specificity is not only related to the type of target but also relies heavily on the enhanced permeability and retention (EPR) effect, which is greatly influenced by the

physical and chemical properties of the photosensitizers. Recently, several studies have utilized the living attributes of microorganisms to develop new specific anti-tumor approaches. Compared with traditional therapies, treatments using microorganisms and their derivatives have the advantages of reduced systemic toxicity, active mobility, precise accurate tumor self-propulsion and penetration, and flexible adaptation to the tumor microenvironment to evoke innate immunity.[125,126] Nevertheless, excessive immune responses can also lead to inflammation; thus, it is necessary to balance appropriate immune responses with severe inflammation. Despite all efforts to improve the aggregation of photosensitizers at the tumor site, tumor-specific therapy remains in the early stages. In the future, more efforts should be made to develop different targeting strategies through pathological studies according to the heterogeneity of the disease; in addition, multiple targeting strategies may also improve the anti-tumor efficiency.

(3) Due to difficulties in the preparation of photosensitizers excited at a specific range of wavelengths and the high expense of NIR-II-related instruments, currently, most NIR-II photosensitizers still use excitation at the 1064 nm wavelength, ignoring the study of other wavelength excitation photosensitizers. Therefore, the joint efforts of researchers in various fields to develop photosensitizers that are excited by other wavelengths and the relevant equipment are both required. In addition, recent evidence suggests that NIR-II light has a lower phototoxicity, a higher maximum permissible exposure (MPE), and a deeper tissue-penetration depth. However, the lower energy of the NIR-II photons results in less efficient ROS generation. Therefore, it is urgent to develop photosensitizers with a high light-conversion efficiency. Moreover, research into the antitumor effects of NIR-II photosensitizers remains in its infancy, and the phototoxicity of NIR-II light laser needs to be evaluated further in clinical applications.

(4) In preclinical studies, mouse xenograft cancer models are commonly used, which are significantly different from real human biological and physiological parameters, leading to failures in clinical translation. In order to better evaluate the clinical treatment effects, the following methods can be used. Firstly, the selection of large animal models such as primates should be added to *in vivo* evaluation studies. Secondly, a better computational model could more accurately evaluate drug accumulation and pharmacokinetics, effectively assessing differences between the preclinical and clinical efficacy. Furthermore, organ-on-chip models are another method to address the poor *in vitro–in viv*o correlation of photosensitizers, which is similar to human physiological functions, thus obtaining more accurate drug response data.[127,128] Finally, the long-term chronic toxicity of NIR-II photosensitizers is a key issue that affects their clinical application, and needs further evaluation.

Based on the above discussion, current high-efficiency NIR-II photosensitizers remain scarce, and will bring new hotspots to phototherapy research. Besides, the clinical application of NIR-II PDT still needs to be explored further, which requires favourable collaboration between interdisciplinary fields, including chemistry, materials science, nanoscience, and pharmaceuticals. In short, we believe that rapid progress on NIR-II-activated photosensitizers will advance new horizons in precision medicine, especially for the accurate treatment of cancer.

Conflicts of interest

There are no conflicts to declare.

Acknowledgements

This work was funded by the National Natural Science Foundation of China (No. 32001010) and the Beijing Institute of Technology Science, Technology Innovation Plan Project (2022CX01029), and The Young Elite Scientist Sponsorship Program of Beijing Association for Science and Technology (No. BYESS2021162). J. Z. would like to thank Biological & Medical Engineering Core Facilities (Beijing Institute of Technology) for providing advanced equipment.

References

1 L. Huang, S. Zhao, F. Fang, T. Xu, M. Lan and J. Zhang, *Biomaterials*, 2021, **268**, 120557.
2 Y. Zhang, F. Fang, L. Li and J. Zhang, *ACS Biomater. Sci. Eng.*, 2020, **6**, 4816–4833.
3 J. Chen, T. Fan, Z. Xie, Q. Zeng, P. Xue, T. Zheng, Y. Chen, X. Luo and H. Zhang, *Biomaterials*, 2020, **237**, 119827.
4 C. Liang, X. Zhang, Z. Wang, W. Wang, M. Yang and X. Dong, *J. Mater. Chem. B*, 2020, **8**, 4748–4763.
5 C. Hopper, *Lancet Oncol.*, 2000, **1**, 212–219.
6 R. Vankayala and K. C. Hwang, *Adv. Mater.*, 2018, **30**, 1706320.
7 Y. Wan, G. Lu, J. Zhang, Z. Wang, X. Li, R. Chen, X. Cui, Z. Huang, Y. Xiao, J. Chelora, W. Zhang, Y. Liu, M. Li, H.-Y. Xie and C.-S. Lee, *Adv. Funct. Mater.*, 2019, **29**, 1903436.
8 J. Zhang, F. Fang, B. Liu, J.-H. Tan, W.-C. Chen, Z. Zhu, Y. Yuan, Y. Wan, X. Cui, S. Li, Q.-X. Tong, J. Zhao, X.-M. Meng and C.-S. Lee, *ACS Appl. Mater. Interfaces*, 2019, **11**, 41051–41061.
9 F. Fang, S. Wang, Y. Song, M. Sun, W.-C. Chen, D. Zhao and J. Zhang, *Nat. Commun.*, 2023, **14**, 1660.
10 T. Yano, T. Minamide, K. Takashima, K. Nakajo, T. Kadota and Y. Yoda, *J. Clin. Med.*, 2021, **10**, 2785.
11 R. R. Allison, G. H. Downie, R. Cuenca, X.-H. Hu, C. J. H. Childs and C. H. Sibata, *Photodiagn. Photodyn. Ther.*, 2004, **1**, 27–42.
12 R. R. Allison and C. H. Sibata, *Photodiagn. Photodyn. Ther.*, 2010, **7**, 61–75.
13 S. Das, M. Tiwari, D. Mondal, B. R. Sahoo and D. K. Tiwari, *J. Mater. Chem. B*, 2020, **8**, 10897–10940.
14 S. Yin, J. Song, D. Liu, K. Wang and J. Qi, *Molecules*, 2022, **27**, 6649.
15 H. Dai, Q. Shen, J. Shao, W. Wang, F. Gao and X. Dong, *Innovation*, 2021, **2**, 100082.
16 X. Zhao, J. Liu, J. Fan, H. Chao and X. Peng, *Chem. Soc. Rev.*, 2021, **50**, 4185–4219.

17 L. Zhu, M. Luo, Y. Zhang, F. Fang, M. Li, F. An, D. Zhao and J. Zhang, *Coord. Chem. Rev.*, 2023, **475**, 214875.
18 Y. Liu, J. Huang and J. Liu, *J. Mater. Chem. B*, 2022, **10**, 7760–7771.
19 P. Ran, T. Xia, H. Zheng, F. Lei, Z. Zhang, J. Wei and X. Li, *Acta Biomater.*, 2023, **155**, 292–303.
20 M. Qiu, D. Wang, H. Huang, T. Yin, W. Bao, B. Zhang, Z. Xie, N. Xie, Z. Wu, C. Ge, Q. Wang, M. Gu, H. L. Kutscher, L. Liu, S. Bao, P. N. Prasad and H. Zhang, *Adv. Mater.*, 2021, **33**, 2102562.
21 Y. Yu, S. Wu, L. Zhang, S. Xu, C. Dai, S. Gan, G. Xie, G. Feng and B. Z. Tang, *Biomaterials*, 2022, **280**, 121255.
22 X. Li, F. Fang, B. Sun, C. Yin, J. Tan, Y. Wan, J. Zhang, P. Sun, Q. Fan, P. Wang, S. Li and C.-S. Lee, *Nanoscale Horiz.*, 2021, **6**, 177–185.
23 X. Cui, G. Lu, S. Dong, S. Li, Y. Xiao, J. Zhang, Y. Liu, X. Meng, F. Li and C.-S. Lee, *Mater. Horiz.*, 2021, **8**, 571–576.
24 Y. Wan, G. Lu, W.-C. Wei, Y.-H. Huang, S. Li, J.-X. Chen, X. Cui, Y.-F. Xiao, X. Li, Y. Liu, X.-M. Meng, P. Wang, H.-Y. Xie, J. Zhang, K.-T. Wong and C.-S. Lee, *ACS Nano*, 2020, **14**, 9917–9928.
25 X. Cui, J. Zhang, Y. Wan, F. Fang, R. Chen, D. Shen, Z. Huang, S. Tian, Y. Xiao, X. Li, J. Chelora, Y. Liu, W. Zhang and C.-S. Lee, *ACS Appl. Bio Mater.*, 2019, **2**, 3854–3860.
26 J. Zhang, W. Chen, R. Chen, X.-K. Liu, Y. Xiong, S. V. Kershaw, A. L. Rogach, C. Adachi, X. Zhang and C.-S. Lee, *Chem. Commun.*, 2016, **52**, 11744–11747.
27 M. Tavakkoli Yaraki, B. Liu and Y. N. Tan, *Nanomicro Lett.*, 2022, **14**, 123.
28 J. Xie, Y. Wang, W. Choi, P. Jangili, Y. Ge, Y. Xu, J. Kang, L. Liu, B. Zhang, Z. Xie, J. He, N. Xie, G. Nie, H. Zhang and J. S. Kim, *Chem. Soc. Rev.*, 2021, **50**, 9152–9201.
29 B. Sun, J. N. Bte Rahmat and Y. Zhang, *Biomaterials*, 2022, **291**, 121875.
30 Y. Qian, J. Wang, W. Bu, X. Zhu, P. Zhang, Y. Zhu, X. Fan and C. Wang, *Biomater. Sci.*, 2023, **11**, 704–718.
31 X. Li, J. F. Lovell, J. Yoon and X. Chen, *Nat. Rev. Clin. Oncol.*, 2020, **17**, 657–674.
32 C. Yin, X. Lu, Q. Fan and W. Huang, *View*, 2021, **2**, 20200070.
33 G. Hong, A. L. Antaris and H. Dai, *Nat. Biomed. Eng.*, 2017, **1**, 1–22.
34 X. Zhang, L. An, Q. Tian, J. Lin and S. Yang, *J. Mater. Chem. B*, 2020, **8**, 4738–4747.
35 F. Fang, L. Zhu, M. Li, Y. Song, M. Sun, D. Zhao and J. Zhang, *Adv. Sci.*, 2021, **8**, 2102970.
36 D. Yang, G. Yang, J. Li, S. Gai, F. He and P. Yang, *J. Mater. Chem. B*, 2017, **5**, 4152–4161.
37 F. Fang, Y. Yuan, Y. Wan, J. Li, Y. Song, W.-C. Chen, D. Zhao, Y. Chi, M. Li, C.-S. Lee and J. Zhang, *Small*, 2022, **18**, 2106215.
38 Y. Jiang, P. K. Upputuri, C. Xie, Y. Lyu, L. Zhang, Q. Xiong, M. Pramanik and K. Pu, *Nano Lett.*, 2017, **17**, 4964–4969.
39 Q. Shen, S. Wang, N.-D. Yang, C. Zhang, Q. Wu and C. Yu, *J. Lumin.*, 2020, **225**, 117338.
40 X. Ding, C. H. Liow, M. Zhang, R. Huang, C. Li, H. Shen, M. Liu, Y. Zou, N. Gao, Z. Zhang, Y. Li, Q. Wang, S. Li and J. Jiang, *J. Am. Chem. Soc.*, 2014, **136**, 15684–15693.
41 H. Lin, Z. Lin, K. Zheng, C. Wang, L. Lin, J. Chen and J. Song, *Adv. Optical Mater.*, 2021, **9**, 2002177.
42 Q. Xin, H. Ma, H. Wang and X.-D. Zhang, *Exploration*, 2023, 20220011.
43 K. Wanderi and Z. Cui, *Exploration*, 2022, **2**, 20210097.
44 T. Shi, C. Huang, Y. Li, F. Huang and S. Yin, *Biomaterials*, 2022, **285**, 121535.
45 Y. Ma, Y. Zhang, X. Li, Y. Zhao, M. Li, W. Jiang, X. Tang, J. Dou, L. Lu, F. Wang and Y. Wang, *ACS Nano*, 2019, **13**, 11967–11980.
46 R. Tian, W. Sun, M. Li, S. Long, M. Li, J. Fan, L. Guo and X. Peng, *Chem. Sci.*, 2019, **10**, 10106–10112.
47 D. An, J. Fu, B. Zhang, N. Xie, G. Nie, H. Ågren, M. Qiu and H. Zhang, *Adv. Funct. Mater.*, 2021, **31**, 2101625.
48 C. Xu and K. Pu, *Chem. Soc. Rev.*, 2021, **50**, 1111–1137.
49 Y. Liu, Y. Li, S. Koo, Y. Sun, Y. Liu, X. Liu, Y. Pan, Z. Zhang, M. Du, S. Lu, X. Qiao, J. Gao, X. Wang, Z. Deng, X. Meng, Y. Xiao, J. S. Kim and X. Hong, *Chem. Rev.*, 2022, **122**, 209–268.
50 B. Li, M. Zhao, J. Lin, P. Huang and X. Chen, *Chem. Soc. Rev.*, 2022, **51**, 7692–7714.
51 S. He, J. Song, J. Qu and Z. Cheng, *Chem. Soc. Rev.*, 2018, **47**, 4258–4278.
52 Q. Qu, Z. Zhang, X. Guo, J. Yang, C. Cao, C. Li, H. Zhang, P. Xu, Z. Hu and J. Tian, *J. Nanobiotechnol.*, 2022, **20**, 143.
53 Z. Hu, C. Fang, B. Li, Z. Zhang, C. Cao, M. Cai, S. Su, X. Sun, X. Shi, C. Li, T. Zhou, Y. Zhang, C. Chi, P. He, X. Xia, Y. Chen, S. S. Gambhir, Z. Cheng and J. Tian, *Nat. Biomed. Eng.*, 2020, **4**, 259–271.
54 X. Shi, Z. Zhang, Z. Zhang, C. Cao, Z. Cheng, Z. Hu, J. Tian and N. Ji, *IEEE Trans. Biomed. Eng.*, 2022, **69**, 1889–1900.
55 C. S. Foote, *Photochem. Photobiol.*, 1991, **54**, 659.
56 M. R. Younis, G. He, J. Qu, J. Lin, P. Huang and X.-H. Xia, *Adv. Sci.*, 2021, **8**, 2102587.
57 M. Lan, S. Zhao, W. Liu, C.-S. Lee, W. Zhang and P. Wang, *Adv. Healthcare Mater.*, 2019, **8**, 1900132.
58 Q. Yao, J. Fan, S. Long, X. Zhao, H. Li, J. Du, K. Shao and X. Peng, *Chem*, 2022, **8**, 197–209.
59 M. Hassan, V. G. Gomes, A. Dehghani and S. M. Ardekani, *Nano Res.*, 2018, **11**, 1–41.
60 L. D. Dias, H. H. Buzzá, M. D. Stringasci and V. S. Bagnato, *Photochem*, 2021, **1**, 434–447.
61 R. G. Mendes, A. Bachmatiuk, B. Büchner, G. Cuniberti and M. H. Rümmeli, *J. Mater. Chem. B*, 2013, **1**, 401–428.
62 L. D. Dias and I. S. Mfouo-Tynga, *Small*, 2020, **5**, 53.
63 S. Masoudi Asil, E. D. Guerrero, G. Bugarini, J. Cayme, N. De Avila, J. Garcia, A. Hernandez, J. Mecado, Y. Madero, F. Moncayo, R. Olmos, D. Perches, J. Roman, D. Salcido-Padilla, E. Sanchez, C. Trejo, P. Trevino, M. Nurunnabi and M. Narayan, *View*, 2023, **4**, 20220056.
64 J. Du, N. Xu, J. Fan, W. Sun and X. Peng, *Small*, 2019, **15**, 1805087.
65 B.-P. Jiang, B. Zhou, Z. Lin, H. Liang and X.-C. Shen, *Chem. – Eur. J.*, 2019, **25**, 3993–4004.

66 L. Wang, K. Kang, Y. Ma, F. Zhang, W. Guo, K. Yu, K. Wang, F. Qu and H. Lin, *Chem. Eng. J.*, 2022, **444**, 136512.
67 S. Iravani and R. S. Varma, *Chem. Commun.*, 2022, **58**, 7336–7350.
68 H. Lin, S. Gao, C. Dai, Y. Chen and J. Shi, *J. Am. Chem. Soc.*, 2017, **139**, 16235–16247.
69 H. Xiang, H. Lin, L. Yu and Y. Chen, *ACS Nano*, 2019, **13**, 2223–2235.
70 Z. Guo, S. Chen, Z. Wang, Z. Yang, F. Liu, Y. Xu, J. Wang, Y. Yi, H. Zhang, L. Liao, P. K. Chu and X.-F. Yu, *Adv. Mater.*, 2017, **29**, 1703811.
71 Y. Zhang, S. Li, X. Fang, B. Miao, Y. Wang, J. Liu, G. Nie and B. Zhang, *Nanophotonics*, 2022, **11**, 5189–5204.
72 R. R. Arvizo, S. Bhattacharyya, R. A. Kudgus, K. Giri, R. Bhattacharya and P. Mukherjee, *Chem. Soc. Rev.*, 2012, **41**, 2943–2970.
73 M. Kim, J.-H. Lee and J.-M. Nam, *Adv. Sci.*, 2019, **6**, 1900471.
74 D. Yang, F. Deng, D. Liu, B. He, B. He, X. Tang and Q. Zhang, *Asian J. Pharm.*, 2019, **14**, 349–364.
75 P. K. Jain, X. Huang, I. H. El-Sayed and M. A. El-Sayed, *Acc. Chem. Res.*, 2008, **41**, 1578–1586.
76 N. Kuthala, M. Shanmugam, X. Kong, C.-S. Chiang and K. C. Hwang, *Nanoscale Horiz.*, 2022, **7**, 589–606.
77 Y. Huang, L. Dai, L. Song, L. Zhang, Y. Rong, J. Zhang, Z. Nie and T. Chen, *ACS Appl. Mater. Interfaces*, 2016, **8**, 27949–27955.
78 J. Hu, Z. Wang and J. Li, *Sensors*, 2007, **7**, 3299–3311.
79 Q. Chen, J. Chen, Z. Yang, L. Zhang, Z. Dong and Z. Liu, *Nano Res.*, 2018, **11**, 5657–5669.
80 Q. Wang, B. Qu, J. Li, Y. Liu, J. Dong, X. Peng and R. Zhang, *ACS Appl. Mater. Interfaces*, 2022, **14**, 4980–4994.
81 L. Jin, S. Shen, Y. Huang, D. Li and X. Yang, *Biomaterials*, 2021, **268**, 120582.
82 Y. Zhao, S.-B. Wang, A.-Z. Chen and R. K. Kankala, *Coord. Chem. Rev.*, 2022, **472**, 214765.
83 Z. Bao, X. Liu, Y. Liu, H. Liu and K. Zhao, *Asian J. Pharm.*, 2016, **11**, 349–364.
84 L. Wang, K. Kang, H. Hou, Y. Ma, K. Yu, F. Qu and H. Lin, *J. Colloid Interface Sci.*, 2022, **625**, 145–157.
85 W. A. Murray and W. L. Barnes, *Adv. Mater.*, 2007, **19**, 3771–3782.
86 C. Zhu, Z. Ding, Z. Guo, X. Guo, A. Yang, Z. Li, B.-P. Jiang and X.-C. Shen, *Biomater. Sci.*, 2020, **8**, 6515–6525.
87 G. Song, J. Shen, F. Jiang, R. Hu, W. Li, L. An, R. Zou, Z. Chen, Z. Qin and J. Hu, *ACS Appl. Mater. Interfaces*, 2014, **6**, 3915–3922.
88 G. Song, J. Hao, C. Liang, T. Liu, M. Gao, L. Cheng, J. Hu and Z. Liu, *Angew. Chem. Int. Ed.*, 2016, **55**, 2122–2126.
89 Y. Wang, N. Gong, Y. Li, Q. Lu, X. Wang and J. Li, *J. Am. Chem. Soc.*, 2020, **142**, 1735–1739.
90 W. Yin, T. Bao, X. Zhang, Q. Gao, J. Yu, X. Dong, L. Yan, Z. Gu and Y. Zhao, *Nanoscale*, 2018, **10**, 1517–1531.
91 J. Li, H.-L. Peng, C. Wen, P. Xu, X.-C. Shen and C. Gao, *Langmuir*, 2022, **38**, 5502–5514.
92 H. S. Naher, B. A. H. Al-Turaihi, S. H. Mohammed, S. M. Naser, M. A. Albark, H. A. Madlool, H. A. M. Al-Marzoog and A. Turki Jalil, *J. Drug Delivery Sci. Technol.*, 2023, **80**, 104175.
93 R. Rafique, S. K. Kailasa and T. J. Park, *Trends Analyt. Chem.*, 2019, **120**, 115646.
94 J. F.-C. Loo, Y.-H. Chien, F. Yin, S.-K. Kong, H.-P. Ho and K.-T. Yong, *Coord. Chem. Rev.*, 2019, **400**, 213042.
95 G. Zhang, Z. Wu, Y. Yang, J. Shi, J. Lv, Y. Fang, Z. Shen, Z. Lv, P. Li, X. Yao, W. Chen, X. Wei, P. K. Chu and X. Zhang, *Chem. Eng. J.*, 2022, **428**, 131155.
96 S. Bi, Z. Deng, J. Huang, X. Wen and S. Zeng, *Adv. Mater.*, 2023, **35**, 2207038.
97 K. Wang, Y. Xu, Z. Chen, H. Li, R. Hu, J. Qu, Y. Lu and L. Liu, *Nanophotonics*, 2022, **11**, 5089–5100.
98 H. Bian, D. Ma, X. Zhang, K. Xin, Y. Yang, X. Peng and Y. Xiao, *Small*, 2021, **17**, 2100398.
99 S. Wang, X. Wang, L. Yu and M. Sun, *Photodiagn. Photodyn. Ther.*, 2021, **34**, 102254.
100 W. Park, S. Cho, J. Han, H. Shin, K. Na, B. Lee and D.-H. Kim, *Biomater. Sci.*, 2018, **6**, 79–90.
101 J. Luo, Z. Xie, J. W. Y. Lam, L. Cheng, H. Chen, C. Qiu, H. S. Kwok, X. Zhan, Y. Liu, D. Zhu and B. Z. Tang, *Chem. Commun.*, 2001, 1740–1741.
102 Z. Zhuang, F. Bu, W. Luo, H. Peng, S. Chen, R. Hu, A. Qin, Z. Zhao and B. Z. Tang, *J. Mater. Chem. C*, 2017, **5**, 1836–1842.
103 Y. Li, Z. Zhao, J. Zhang, R. T. K. Kwok, S. Xie, R. Tang, Y. Jia, J. Yang, L. Wang, J. W. Y. Lam, W. Zheng, X. Jiang and B. Z. Tang, *Adv. Funct. Mater.*, 2018, **28**, 1804632.
104 Z. Zhao, H. Zhang, J. W. Y. Lam and B. Z. Tang, *Angew. Chem., Int. Ed.*, 2020, **59**, 9888–9907.
105 Y. Wang, S. Xu, L. Shi, C. Teh, G. Qi and B. Liu, *Angew. Chem., Int. Ed.*, 2021, **60**, 14945–14953.
106 S. Wang, X. Li, S. Y. Chong, X. Wang, H. Chen, C. Chen, L. G. Ng, J.-W. Wang and B. Liu, *Adv. Mater.*, 2021, **33**, 2007490.
107 S. Wang, H. Chen, J. Liu, C. Chen and B. Liu, *Adv. Funct. Mater.*, 2020, **30**, 2002546.
108 J.-S. Ni, P. Zhang, T. Jiang, Y. Chen, H. Su, D. Wang, Z.-Q. Yu, R. T. K. Kwok, Z. Zhao, J. W. Y. Lam and B. Z. Tang, *Adv. Mater.*, 2018, **30**, 1805220.
109 Y. Gao, G. Feng, T. Jiang, C. Goh, L. Ng, B. Liu, B. Li, L. Yang, J. Hua and H. Tian, *Adv. Funct. Mater.*, 2015, **25**, 2857–2866.
110 J. Zhang, W. Chen, S. Kalytchuk, K. F. Li, R. Chen, C. Adachi, Z. Chen, A. L. Rogach, G. Zhu, P. K. N. Yu, W. Zhang, K. W. X. Shi, Z. Zhang, Z. Zhang, C. Cao, Z. Cheng, Z. Hu, J. Tian and N. Ji, *IEEE Trans. Biomed. Eng.*, 2022, **69**, 1889–1900.
111 Z. He, Y. Gao, H. Zhang, Y. Xue, F. Meng and L. Luo, *Adv. Healthcare Mater.*, 2021, **10**, 2101056.
112 N. Yu, L. Zhao, D. Cheng, M. Ding, Y. Lyu, J. Zhao and J. Li, *J. Colloid Interface Sci.*, 2022, **619**, 219–228.
113 C. Yin, X. Li, G. Wen, B. Yang, Y. Zhang, X. Chen, P. Zhao, S. Li, R. Li, L. Wang, C.-S. Lee and L. Bian, *Biomaterials*, 2020, **232**, 119684.

114 C. Yin, X. Zhen, Q. Fan, W. Huang and K. Pu, *ACS Nano*, 2017, **11**, 4174–4182.
115 J. Li, J. Rao and K. Pu, *Biomaterials*, 2018, **155**, 217–235.
116 K. Wen, H. Tan, Q. Peng, H. Chen, H. Ma, L. Wang, A. Peng, Q. Shi, X. Cai and H. Huang, *Adv. Mater.*, 2022, **34**, 2108146.
117 J. Wen, K. Yang, J. Huang and S. Sun, *Mater. Des.*, 2021, **198**, 109298.
118 Y. Yang, T. Hu, Y. Bian, F. Meng, S. Yu, H. Li, Q. Zhang, L. Gu, X. Weng, C. Tan and R. Liang, *Adv. Mater.*, 2023, **35**, 2211205.
119 S. L. Suib, *Chem. Rec.*, 2017, **17**, 1169–1183.
120 V. Cauda and G. Canavese, *Pharmaceutics*, 2020, **12**, 1108.
121 G. Wan, X. Chen, J. Chen, R. Gou, H. Wang, S. Liu, M. Zhang, H. Chen, D. Wang and Q. Zhang, *Biomater. Sci.*, 2023, **11**, 1876–1894.
122 W. Zhang, M. Wang, B. Liu, M. Yuan, Z. Yang, J. Tan, P. A. Ma and J. Lin, *Chem. Eng. J.*, 2023, **460**, 141818.
123 M. Souri, M. Soltani, F. Moradi Kashkooli, M. Kiani Shahvandi, M. Chiani, F. S. Shariati, M. R. Mehrabi and L. L. Munn, *Mater. Today Bio.*, 2022, **13**, 100208.
124 D. Rosenblum, N. Joshi, W. Tao, J. M. Karp and D. Peer, *Nat. Commun.*, 2018, **9**, 1410.
125 Q.-W. Chen, J.-Y. Qiao, X.-H. Liu, C. Zhang and X.-Z. Zhang, *Chem. Soc. Rev.*, 2021, **50**, 12576–12615.
126 W. Wu, Y. Pu, S. Gao, Y. Shen, M. Zhou, H. Yao and J. Shi, *Nanomicro Lett.*, 2022, **14**, 220.
127 B. Zhang, A. Korolj, B. F. L. Lai and M. Radisic, *Nat. Rev. Mater.*, 2018, **3**, 257–278.
128 J. Zhu, L. Ji, Y. Chen, H. Li, M. Huang, Z. Dai, J. Wang, D. Xiang, G. Fu, Z. Lei and X. Chu, *Cell Death Discovery*, 2023, **9**, 72.